ResearchGate

See discussions, stats, and author profiles for this publication at: https://www.researchgate.net/publication/231649426

Quantitative Prediction of Two-Photon Absorption Cross Section Based on Linear Spectroscopic Properties†

ARTICLE *in* THE JOURNAL OF PHYSICAL CHEMISTRY C · MAY 2008

Impact Factor: 4.77 · DOI: 10.1021/jp800104q

CITATIONS
36

READS
29

9 AUTHORS, INCLUDING:

Aleksander Rebane
Montana State University
261 PUBLICATIONS **4,774** CITATIONS
SEE PROFILE

Mikhail Drobizhev
Montana State University
162 PUBLICATIONS **3,649** CITATIONS
SEE PROFILE

Benjamin D. Reeves
Montana State University
23 PUBLICATIONS **433** CITATIONS
SEE PROFILE

Charles W Spangler
Montana State University
175 PUBLICATIONS **3,831** CITATIONS
SEE PROFILE

Available from: Benjamin D. Reeves
Retrieved on: 26 January 2016

Quantitative Prediction of Two-Photon Absorption Cross Section Based on Linear Spectroscopic Properties†

Aleksander Rebane,[‡,||,⊥] Nikolay S. Makarov,[||] Mikhail Drobizhev,[||] Brenda Spangler,[*,#] E. Scott Tarter,[#] Benjamin D. Reeves,[#] Charles W. Spangler,[§,∇,○] Fanqing Meng,[○] and Zhiyong Suo[||]

Department of Physics, Montana State University, Bozeman, Montana 59717, National Institute of Chemical Physics and Biophysics, Tallinn, EE 12618, Estonia, Sensopath Technologies, Inc., Bozeman, Montana 59715, Department of Chemistry and Biochemistry, Montana State University, Bozeman, Montana 59717, and MPA Technologies, Inc., Bozeman, Montana 59715

Received: January 6, 2008; Revised Manuscript Received: February 28, 2008

We study two-photon absorption (2PA) spectra in a broad class of organic dye molecules, such as substituted diphenylaminostilbenes, push−pull porphyrins, and carbazol-substituted stilbenes. We show, for the first time, that the 2PA cross section in the lowest-energy dipole-allowed transition may be predicted with better than 50% absolute accuracy based solely on the molecular parameters obtained from linear spectroscopic measurements.

1. Introduction

Designing molecules for two-photon fluorescence microscopy,[1] and other emerging applications of two-photon absorption (2PA) including 3D optical memory,[2–5] nanofabrication,[6] optical power limiting,[7] and photodynamic therapy,[8,9] requires knowledge of underlying structure−property relationships for 2PA cross sections (σ_2) in a broad range of different chromophores. Usually, such information is obtained from direct quantitative measurement of the nonlinear absorption. This task is often tedious and requires special wavelength-tunable short-pulsed lasers. Alternatively, 2PA spectra and σ_2 values may be forecast on the basis of theoretical quantum-chemical calculations.[10–13] In this case, one computes molecular transition and permanent dipole moments with the associated transition frequencies and then uses these values in perturbation expansion formulas (or equivalent relations) to obtain the nonlinear-optical properties. Although quantum-chemical methods have an advantage that they can account for many excited states, they are also limited by finite computational accuracy. If the number of atoms involved in the calculation becomes large (e.g., over 20), then the quantitative prediction of the 2PA cross sections becomes less accurate.

Here, we are proposing an alternative approach, where the 2PA cross sections are found based on the quantities determined solely from linear (one-photon) measurements. In this way, one may be able to avoid the limitations of quantum-chemical calculations as well as circumvent complicated nonlinear-optical experiments.

Previously, two, three, and four energy level models have been successful in establishing correspondence between theoretical and experimental 2PA cross section values.[14–20] It was shown that some molecules, especially those lacking center of symmetry, may be qualitatively described by the two-level model.[16] At the same time, in symmetrical molecules and in the molecules with small permanent dipole moments, the 2PA cross sections were better approximated with three- or four-level models, which does require accounting for high-energy excited states.[16–20] Scaling of the maximum 2PA cross section with an effective number of electrons contributing to the nonlinear response has been discussed in ref 21.

Here we focus on the lowest-energy dipole-allowed transition in a selection of organic fluorophores with different degrees of dipolar character, including substituted diphenylaminostilbenes, push−pull porphyrins, and carbazol-substituted stilbenes. If we may assume that the 2PA is described by the two-level model, then there are only two key parameters that need to be evaluated: the permanent dipole moment difference between the ground and the excited state and the transition dipole moment from the ground state to the excited state. We determine both dipole moment values by using standard spectroscopic techniques: The transition dipole moment is directly related to the molar extinction, while the permanent dipole moment difference may be found from solvent-specific Stokes shifts.[22,23] We evaluate the corresponding σ_2 from the perturbation expansion formula, taking into account absorption line shape and local field correction. The same 2PA cross sections are also measured directly by the femtosecond fluorescence−excitation method, showing a remarkably good coincidence with the predicted values.

2. Theoretical Background

The interaction of a two-level molecule with applied external electric field, $\vec{E}(t)$, is described by the density matrix equation of motion:[24,25]

† Part of the "Larry Dalton Festschrift".

* Corresponding author. Phone: (406) 587-6338; fax: 406-585-8390; e-mail: brenda.spangler@sensopath.com.

‡ Phone: (406)-994-7831; fax: (406)-994-4452; e-mail: rebane@physics.montana.edu.

§ Phone: 406-585-8192; fax: 406-585-8390; e-mail: spangler.charles@gmail.com.

|| Department of Physics, Montana State University.

⊥ National Institute of Chemical Physics and Biophysics.

Sensopath Technologies, Inc.

∇ Department of Chemistry and Biochemistry, Montana State University.

○ MPA Technologies, Inc.

10.1021/jp800104q CCC: $40.75 © 2008 American Chemical Society
Published on Web 05/22/2008

$$\begin{cases} \dfrac{d\rho_{11}}{dt} = \dfrac{2\vec{\mu}_{01}\cdot\vec{E}(t)\mathrm{Im}\rho_{01}}{\hbar} - \dfrac{\rho_{11}}{T_1} \\ \dfrac{d\mathrm{Re}\rho_{01}}{dt} = \left(\dfrac{\Delta\vec{\mu}_{01}\cdot\vec{E}(t)}{\hbar} - \omega_{10}\right)\mathrm{Im}\rho_{01} - \dfrac{\mathrm{Re}\rho_{01}}{T_2} \\ \dfrac{d\mathrm{Im}\rho_{01}}{dt} = -\left(\dfrac{\Delta\vec{\mu}_{01}\cdot\vec{E}(t)}{\hbar} - \omega_{10}\right)\mathrm{Re}\rho_{01} - \dfrac{\vec{\mu}_{01}\cdot\vec{E}(t)(2\rho_{11}-1)}{\hbar} - \dfrac{\mathrm{Im}\rho_{01}}{T_2} \end{cases} \quad (1)$$

where ρ_{01} is the complex off-diagonal density matrix element, ρ_{11} is the population of the excited state, ω_{10} is the resonance transition frequency, and $\hbar$ is Planck's constant. The set of molecular parameters includes the following: $\vec{\mu}_{01}$, transition dipole moment; $\Delta\vec{\mu}_{01}$, permanent dipole moment difference in the ground and excited states; and T_1 and T_2, decay times of the excited-state population and of the coherence between the two states, respectively. Note that rotating wave approximation is not used here.

Suppose the molecule is illuminated with a brief Gaussian-shaped pulse of carrier frequency, ω, and duration, τ_p, such that the pulse duration is much less than the excited-state energy decay time, $\tau_p \ll T_1$. The probability that the molecule absorbs two photons simultaneously (or one photon in case of 1PA) is directly proportional to the population of the excited state, measured shortly after the pulse. Figure 1 presents the excited-state population, calculated as a function of the pulse carrier frequency. If $\Delta\mu_{01} = 0$, then only the 1PA resonance is observed (dashed line in Figure 1). If $\Delta\mu_{01} \neq 0$, then the 2PA resonance appears at frequency $\omega_{01}/2$. We note that the Lorentzian line shape follows from the exponential relaxation terms in eq 1. In reality, especially in the case of organic molecules, the 1PA falls off much more rapidly with increasing frequency detuning. Figure 1a shows that at the pulse peak intensity used in this model calculation the 2PA increases linearly with I^2, indicating the absence of saturation. Under these conditions, the two-photon cross section can be found from the excited-state population as follows:

$$\sigma_2 = \frac{4h^2\nu^2}{I^2\tau_p}\sqrt{\frac{2\ln 2}{\pi}}(\rho_{11} - \rho_{11}^{1PA}) \quad (2)$$

where ρ_{11}^{1PA} is the excited-state population occurring due to the Lorentzian wing of the one-photon resonance. In Figure 1b, the 2PA line shape (after appropriate scaling of the frequency axis) is superimposed with the Lorentzian line shape of the 1PA resonance, showing that the two line shapes essentially coincide. Below this fact is used to verify if a two-level description of 2PA is applicable. Furthermore, if the measured 1PA line shape is Lorentzian, then we may expect the same line shape also for the 2PA. In practice, the absorption line shapes are often much more involved. The spectra may include multiple overlapping vibronic transitions, as well as inhomogeneous broadening. The implications of the line shape on the 2PA cross section will be discussed below.

In the limit of low intensity, $\rho_{11} \ll 1$, the density matrix eq 1 may be simplified to resemble the classical equation of motion of a slightly anharmonic dipole oscillator:

$$\ddot{\rho}_{01} + \left[\frac{\Delta\vec{\mu}_{01}\cdot\vec{E}(t)}{\hbar} - \omega_{10}\right]^2\rho_{01} + \frac{\rho_{01}}{T_2} = -\frac{\vec{\mu}_{01}\cdot\vec{E}(t)\omega_{10}}{\hbar} \quad (3)$$

The term enclosed in the square brackets may be interpreted as instantaneous resonance transition frequency. If the permanent dipole moment difference is not zero, then the transition is modulated at the optical frequency, leading to the nonlinear absorption resonance at $\omega_{01}/2$.

In the following quantitative analysis, we use a more customary analytical expression for the 2PA cross section, which is obtained from the perturbation theory:[15,16]

$$\sigma_2 = \frac{2(2\pi)^4 f^4}{15(nch)^2}|\vec{\mu}_{01}|^2|\Delta\vec{\mu}_{01}|^2(2\ \cos^2\beta + 1)g(2\nu) \quad (4)$$

where β is the angle between the dipole moments $\vec{\mu}_{01}$ and $\Delta\vec{\mu}_{01}$, f is the local field factor, n is the refractive index, c is the

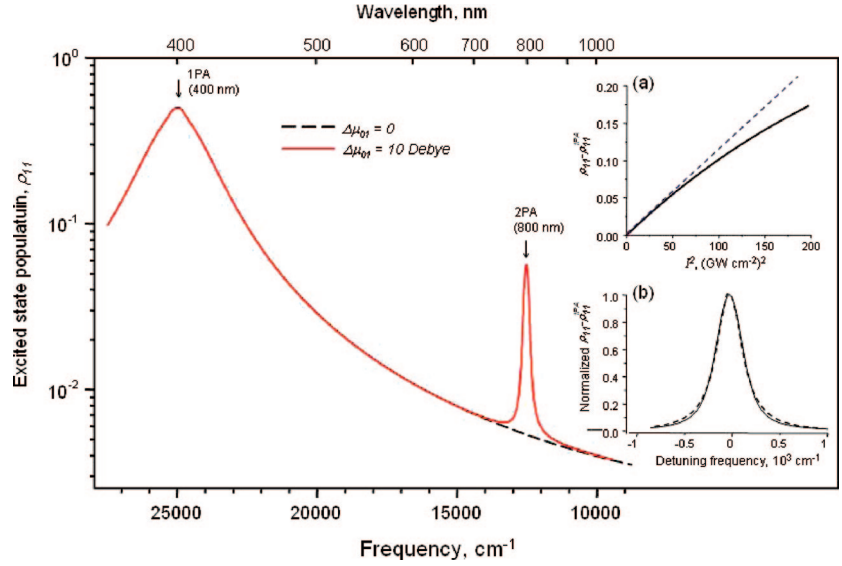

Figure 1. Numerical simulation of 2PA in the two-level system. Main figure (note log scale of vertical axis); solid line, excited-state population as a function of the pulse carrier frequency (parameters used in the calculation: $T_1 = 1600$ fs, $T_2 = 50$ fs, $\tau_p = 100$ fs, $\omega_{01}/2\pi c = 25\,000$ cm^{-1}, $\mu_{01} = 10$ D, $\Delta\vec{\mu}_{01} = 20$ D, pulse peak intensity, $I = 20$ GW cm^{-2}); Dashed line, the same for $\Delta\vec{\mu}_{01} = 0$. Insets: (a) Saturation of the 2PA-induced excited-state population at $\omega_{01}/2$ (solid line) as compared to I^2-dependence (dashed line). (b) Comparison between the 2PA line shape (solid line) and Lorentzian 1PA line shape (dashed line).

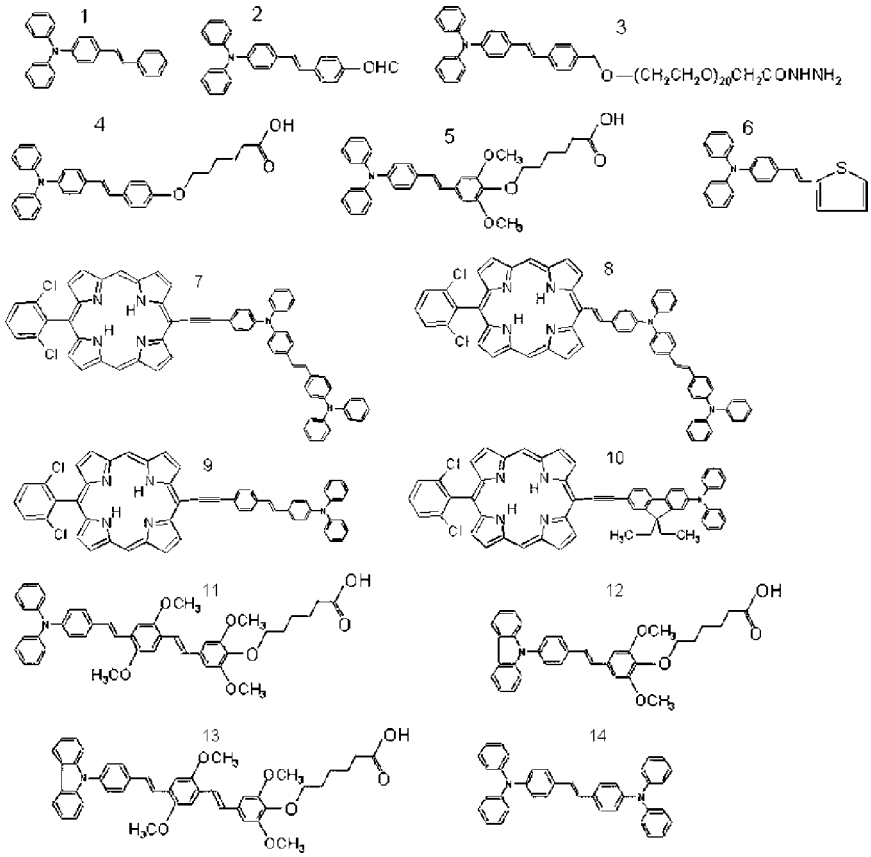

Figure 2. Chemical structures of the compounds studied: **1**−**6** and **11**−**14** are substituted diphenylaminostilbenes; **7**−**10** are meso-DPAS and BDPAS-substituted porphyrins.

speed of light in vacuum, and $g(2\nu)$ is the normalized line shape function

$$\int g(2\nu)d2\nu = 1 \tag{5}$$

Assuming that the 2PA line shape coincides with that of 1PA,[16] one can obtain

$$|\vec{\mu}_{01}|^2 g(\bar{\nu}_{01}) = \frac{3\times 10^3 \ln 10\, hc\varepsilon(\bar{\nu}_{01})n}{(2\pi)^3 N_A \bar{\nu}_{01} f^2} \tag{6}$$

where $g(\bar{\nu}_{01})$ is the maximum of the normalized line shape function, $\bar{\nu}_{01}$ is the frequency of the band maximum (in cm^{-1}), $\varepsilon(\bar{\nu}_{01})$ is the extinction coefficient at the maximum, and N_A is Avogadro's number.

3. Experimental Section

On the basis of their structural properties (Figure 2), the studied compounds may be grouped as follows:

(i) **1**−**6** are substituted diphenylaminostilbenes, of which **2**−**6** are new and **1** was described in refs 26 and 27.

(ii) **7**−**10** are push−pull porphyrins, of which **10** is new and **7**−**9** were studied before in ref 16.

(iii) **11**, **12**, and **13** are new substituted carbazolstilbene, carbazoldistyrylbenzene, and diphenylaminodistyrylbenzene, respectively. (Grouping these compounds separately from I will be clarified later.). **14** is bis-diphenylaminostilbene (BDPAS) and was characterized in literature.[28,29] Synthesis and other details concerning the new compounds are given in the Supporting Information.

3.1. Measurement Techniques. The laser system, along with details of the fluorescence−excitation method, are described in refs 15, 18, and 30. Very briefly, a slightly focused beam of femtosecond optical parametric amplifier (OPA) (TOPAS, Quantronix) is used to excite fluorescence in a solution in a 1-cm spectroscopic cell. The pulse duration was $\tau = 70-100$ fs, the pulse repetition rate was 1 kHz, and the pulse energy was 5−30 μJ. Relative 2PA excitation spectra are obtained by measuring the fluorescence intensity as a function of the OPA wavelength. Absolute 2PA cross sections are determined at selected wavelengths by comparing the intensities of one- and two-photon excited fluorescence under strictly controlled conditions. The 2PA spectra are then calibrated with respect to these absolute values.[18]

For recording of the relative 2PA spectra, compounds **1**−**3** are dissolved in benzene; **4**−**6** and **11**−**13** in *N*,*N*-dimethylformamide; **7**−**9** and **14** in dichloromethane, and **10** in carbon tetrachloride. A 1-mm spectroscopic cell is used to reduce the solvent absorption in the near-IR, as needed.[16] Absolute 2PA cross sections of **1**, **3**−**6**, and **11**−**13** were obtained relative to BDPAS in dichloromethane at $\lambda_{ex} = 650$ nm ($\sigma_2 = 280$ GM[27]) and for **2** at $\lambda_{ex} = 800$ nm ($\sigma_2 = 47$ GM[27]). The absolute cross sections of **7**−**9** were measured relative to free-base tetraphenylporphyrin (H_2TPP) in toluene at $\lambda_{ex} = 1180$ nm ($\sigma_2 = 3.5$ GM[31]). The cross section of **10** was measured at $\lambda_{ex} = 1200$ nm by direct comparison of the 2PA and 1PA fluorescence signals.[15,18]

A PerkinElmer Lambda 900 spectrophotometer is used for UV−vis extinction spectra measurements. A PerkinElmer LS 50B spectrofluorimeter is used for fluorescence emission spectra and fluorescence depolarization measurements. The fluorescence spectra are corrected by accounting for the detector sensitivity as a function of wavelength. Fluorescence anisotropy (r) is

measured according to the standard procedure in L-configuration.[22] The fluorescence spectra, $F(\lambda)$, are converted to frequency units as follows: $F(\{\bar{\nu}\}) = \lambda^2 F(\lambda)$.[22]

Fluorescence Stokes shifts are measured in solvents with different dielectric constant. The Stokes shifts were measured in toluene ($D = 2.4$) vs tetrahydrofuran ($D = 7.58$) for the compounds **3**−**6**, and in octane ($D = 2.0$) vs 2-chlorobutane ($D = 8.06$) for **2**, **8**−**10**. A wider selection of solvents was used for the compounds **1**, **4**, **5**, and **10**−**14**, consisting of n-octane, butyl ether, isobutyl isobutyrate, isobutyl acetate, 2-chlorobutane, and pentanal. Fluorescence decays were measured with a synchro-scan streak camera (Hamamatsu).

4. Results and Discussion

4.1. Direct Measurement of 2PA Spectra and Absolute Cross Sections. Figure 3 a−c shows the 1PA (right vertical scale) and 2PA (left vertical scale) spectra of the molecules. The horizontal scale at the bottom of the graphs corresponds to the transition wavelength (i.e., half of the 2PA laser wavelength), and the scale at the top corresponds to the transition frequency.

All six compounds in group i show qualitatively very similar spectra (Figure 3a). The lowest-energy 1PA absorption consists of a broad peak with the maximum at $\lambda = 410$ nm for compound **2** and $\lambda = 360$−380 nm for compounds **1** and **3**−**6**. In **1**−**4**, the 1PA and 2PA peaks overlap almost within the accuracy of the measurement. Table 1 lists the wavelength of the fluorescence emission maximum, λ_{em}, in benzene.

The width of the peaks in both 1PA and 2PA is about 5000 cm^{-1}. In **5**, the 2PA peak is slightly narrower than the corresponding 1PA peak, while the maxima still coincide. For **6**, the 2PA peak is slightly blue-shifted and narrowed compared to the 1PA peak. In all cases, the 1PA and 2PA profiles are basically the same. Even though the line shapes are closer to Gaussian, we must be dealing here with the same transition. Furthermore, because the main fluorescence peak (Table 1) for all six compounds occurs in the same spectral region as the 1PA peak, we state that the observed peaks correspond to the $S_0 \rightarrow S_1$ transition. A significant difference between the 1PA and 2PA spectra is observed only at shorter wavelengths, $\lambda >$ 310 nm, where 2PA increases sharply, whereas 1PA shows some other weaker peaks. The increase of 2PA may be attributed to resonance enhancement effect.

The peak 2PA cross section values vary from $\sigma_2 = 40$ to 140 GM, which is comparable to those reported for other similar molecules in the lowest dipole-allowed transitions.[10,32−35] The 2PA spectra of **2**−**6** are presented here for the first time.

The spectra of the push−pull porphyrins in group ii are presented in Figure 3b. The main two 1PA peaks are assigned to the Q bands, inherent in tetrapyrroles. Following the notation of ref 16, the longer wavelength band at 650−670 nm is $Q_x^{(1)}$, and the shorter wavelength band at 560−580 nm is $Q_x^{(2)}$. It was shown in ref 16 that $Q_x^{(1)}$ and $Q_x^{(2)}$ bands have parallel transition dipole vectors and that the $Q_x^{(1)}$ band is a superposition of at least three vibronic transitions: purely electronic $Q_x^{(1)}(0-0)$ and two vibronic satellites, $Q_x^{(1)}(0-1)$ and $Q_x^{(1)}(0-1')$. The width of $Q_x^{(1)}$ is about 500−1000 cm^{-1}.

The 2PA spectra of **7**−**10** show relatively narrow peaks that closely match the corresponding 1PA transition. The coincidence is particularly obvious for $Q_x^{(2)}$, where the maximum cross section is in the range $\sigma_2 = 50$−250 GM. Note that the peak 2PA cross section values in the lowest-energy transition ($Q_x^{(1)}$), $\sigma_2 = 5$−20 GM, are about 1 order of magnitude less than the corresponding values in group i. Because of this, and because of the close proximity to a much stronger $Q_x^{(2)}$, the 2PA of $Q_x^{(1)}$ appears more like a shoulder, which is ∼20 nm blue-shifted with respect to the corresponding 1PA. This shift may be attributed to the existence of vibronic satellites, where 2PA may be enhanced compared to that of the 0−0.[16] Here, we may disregard the small shift and consider the vibronic satellites as part of the lowest-energy transition.

Figure 3c shows the spectra of molecules **11**−**14**. The 1PA consist of a strong peak at 300−350 nm, followed by a weaker peak at an shorter wavelengths, 300−320 nm, similar to **5** and **6** in group i. The main fluorescence maximum (Table 1) occurs again in the same spectral region as the 1PA peak, meaning that the last most likely correspond to the $S_0 \rightarrow S_1$ transition. The 2PA spectrum, however, shows a more complex behavior than that in group i. The 2PA peak, coinciding with the lowest-energy $S_0 \rightarrow S_1$ transition, is observed as a broad shoulder on the side of a much stronger transition at the wavelength 300−360 nm. In this respect, molecules in group iii are similar to those in group ii. At the same time, the maximum cross sections in the long-wavelength shoulder are much closer to those in group i, $\sigma_2 \sim 50$−100 GM.

The 2PA spectrum and cross section of **14** agree well with our previous data.[27] It is also known from previous studies that the 2PA peak at 335 nm in compound **14** is due to a higher-energy *g*-parity electronic state.[27,29] A similar peak, which does not correspond to any peak in the 1PA, occurs also in **13** at 365 nm.

4.2. Estimation of 2PA Cross Section from Linear Spectroscopic Measurements. Even though the overall shape and the maximum value of the 2PA spectra varies greatly from one group to another, there is a common feature, corresponding to the lowest-energy 1PA transition. In this section, we will obtain an estimate of the peak value of σ_2 for this transition, by using eqs 4 and 6.

For simplicity, we assume here that the angle between $\vec{\mu}_{01}$ and $\Delta\vec{\mu}_{01}$ is zero, $\beta \approx 0$. The value of $|\Delta\vec{\mu}_{01}|$ can be measured directly via the Stark effect. Here we take a more convenient, albeit indirect, approach where the dipole moment difference is found from the dependence of the fluorescence Stokes shift, $\Delta\bar{\nu}_S$, on the solvent polarity:[23]

$$|\Delta\vec{\mu}_{01}|^2 = \frac{hc\Delta\bar{\nu}_S\, a^3}{\Delta f(D)} \tag{7}$$

where a is the molecular cavity radius, $\Delta f(D) = 2(D_2 - 1) - 2(D_1 - 1)/2D_2 + 1\ 2D_1 + 1$ is the change of the Onsager polarity function between two solvents, where the last have similar refractive index values but different dielectric constants, D_1 and D_2.

Figure 4 shows the solvatochromic shifts measured in a series of solvents for molecules **1**, **4**, **5**, and **10**. The magnitude of the shift increases with the solvent polarity and is described well by a straight line. Table 1 collects the normalized Stokes shifts of the molecules studied. The experimental error of the solvatochromic shift values are about 10% and increases for those molecules where the shift is the smallest. The fact that the Stokes shifts in group ii are much smaller than those in other molecules indicates that the substituted porphyrins have a relatively small permanent dipole moment change.

Determining the value of $|\Delta\vec{\mu}_{01}|$ from the solvatochromic shifts data has been, until recently, subject to considerable uncertainty. Our approach is based on the assumption that the molecular cavity radius equals the hydrodynamic radius of a molecule. The last may be evaluated from the Smolukhovsky−

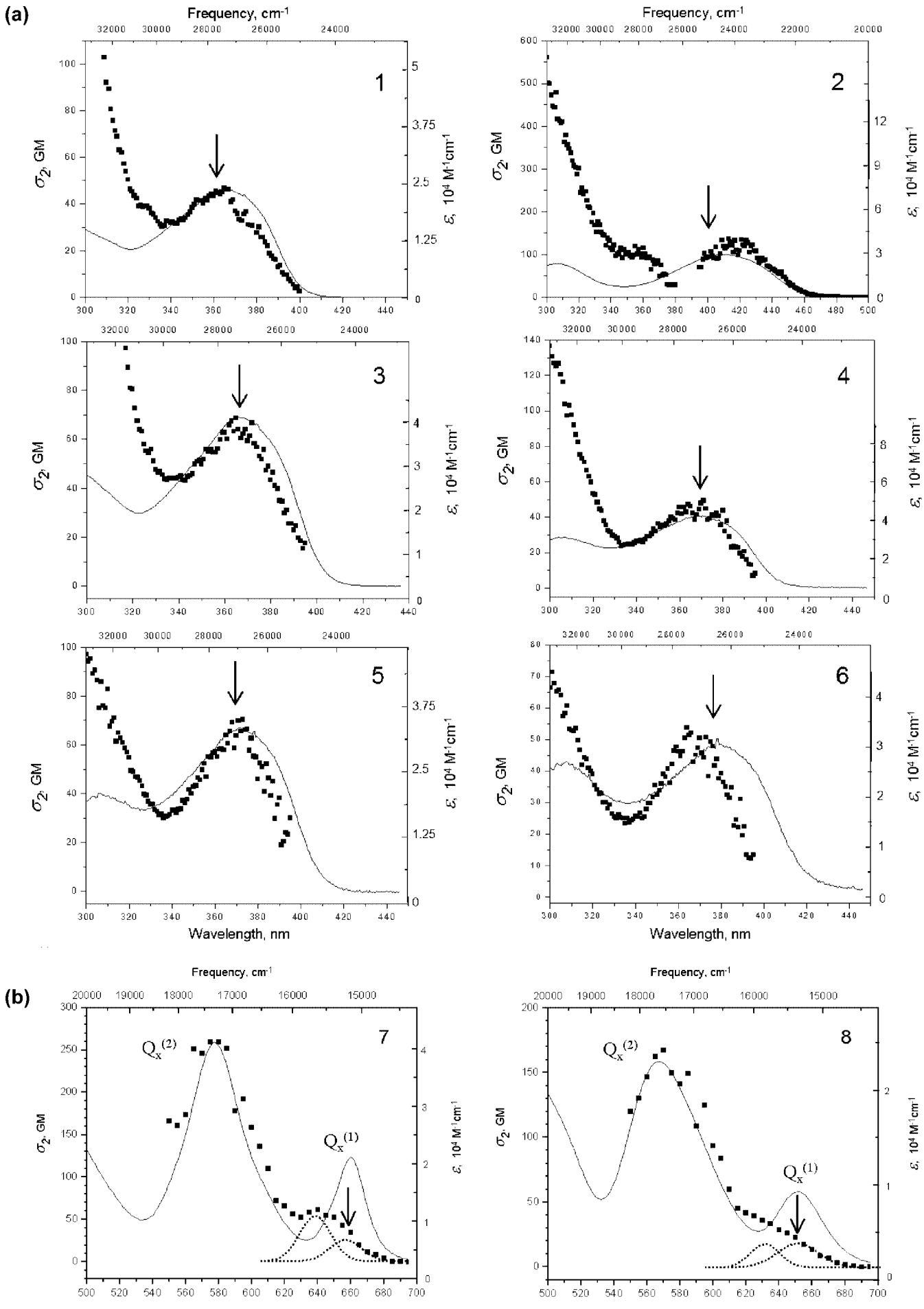

Figure 3. Continued on next page.

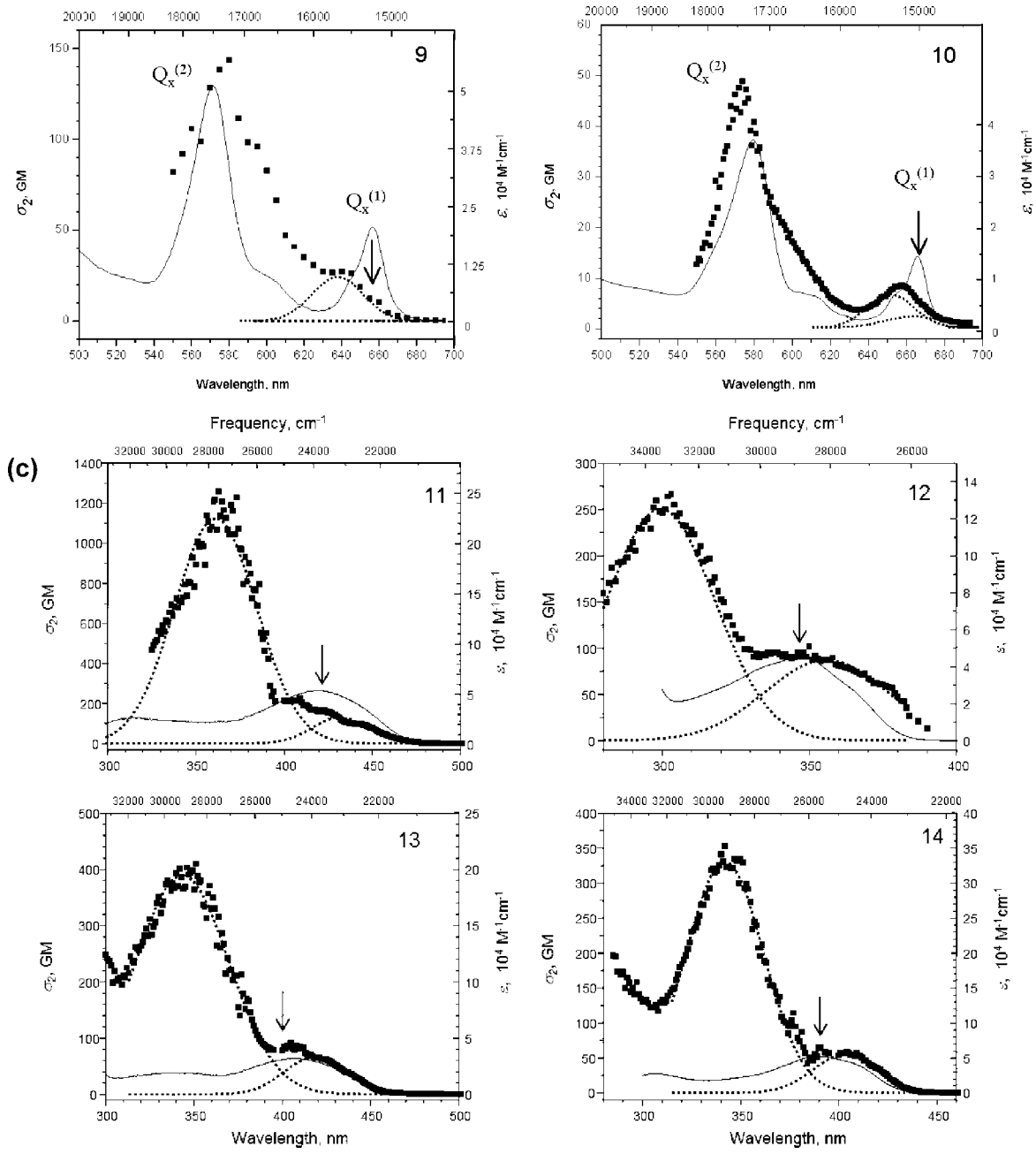

Figure 3. 2PA spectra (rectangles) and 1PA spectra (solid line) of (a) group i, (b) group ii, (c) group iii. Dashed lines show decomposition of the long-wavelength portion of the 2PA spectrum into two Gaussians. The vertical arrow indicates the wavelength, where σ_2^{ex} is evaluated (corresponding to the maximum of the lowest-energy 1PA transition).

Einstein theory of rotational diffusion,[16] which relates the radius to the fluorescence anisotropy:[22]

$$r = 0.4\left(1 + \frac{3\tau_f kT}{4\pi\eta\, a^3}\right)^{-1} \tag{8}$$

where η is the solvent viscosity, τ_f is the fluorescence lifetime, k is the Boltzmann constant, and T is the temperature. Table 1 collects the measured fluorescence lifetimes (in benzene) and fluorescence anisotropies, along with the a values calculated from eq 8, and $|\Delta\vec{\mu}_{01}|$ values calculated from eq 7. We estimate 2% error of the lifetime measurement (Figure 5) and 20% error in the cavity radius. Our values for group i, $|\Delta\vec{\mu}_{01}| = 9-15$ D, correlate well with the previous measurement for **1**, $|\Delta\vec{\mu}_{01}| =$ 11 D.[26]

4.3. Comparison between the Theoretical and Measured 2PA Cross Section Values. Table 1 lists the theoretical cross section values, σ_2^{th}, calculated at the peak of the transition, for two alternative local field models: the Lorentz model, $f_L = (n^2 + 2)/3$, and the Onsager model, $f_O = 3n^2/(2n^2 + 1)$. We estimate that the calculated cross section values have 30% error.

In Figure 6, the horizontal axes shows the 2PA cross sections obtained from the theory with the Onsager local field model, and the vertical axes shows the corresponding experimental values. The experimental cross sections correspond to the wavelength of the lowest-energy 1PA transition maximum, as indicated by the vertical arrow in Figure 3. In group i, the σ_2^{ex} value is obtained directly from the measured 2PA spectra. In groups ii and iii, the 2PA spectrum is decomposed into two Gaussian components, as shown in Figure 3b and c. The σ_2^{ex}

TABLE 1: Summary of the Measured and Calculated Parameters[a]

comp.	R	λ_{em}, nm	τ_f, ns	a, Å	$\Delta\bar{\nu}_S/\Delta f(D)$	$\lvert\Delta\vec{\mu}_{01}\rvert$, D	ϵ, 10^4 $M^{-1}cm^{-1}$	σ_2^{ex}, GM (a)	$\sigma_2^{th(O)}$, GM	$\sigma_2^{th(L)}$, GM
1	0.022	416	1.71	5.3	4260	11.2	2.44	47	55	73
2	0.031	481	1.67	6.0	5330	14.9	3.09	136	136	182
3	0.030	419	1.57	5.8	2010	8.8	4.31	69	60	80
4	0.051	408	1.28	6.6	2990	12.9	4.20	49	79	93
5	0.053	414	1.46	7.0	3230	14.7	3.33	70	95	112
6	0.031	425	1.46	5.7	3080	10.7	3.26	40	26	30
7	0.055	666	2.73	8.3	210	4.5	2.20	20 (35)	17	19
8	0.071	631	1.72	8.2	490	7.1	0.825	16 (23)	16	18
9	0.029	662	3.11	7.1	3	0.4	2.49	0.07 (12)	0.11	0.13
10	0.031	663	2.99	7.2	89	2.6	1.668	2.1 (5.5)	3.7	4.5
11	0.036	386	N.A.	7.0[c]	1870	11.2	5.30	107 (162)	68	80
12	0.065	453	1.45	7.5	520	6.6	4.60	79 (91)	40	47
13	0.069	469	1.88	7.7	800	8.6	3.20	53 (81)	83	97
14	0.036	429	1.15	5.6	890	5.5	5.24	39 (51)	31	36

[a] λ_{em}, r, τ_f, and a are measured in benzene. ϵ and σ_2^{ex} are measured as described in the text. [b] Value in the parentheses is σ_2 from Figure 3 at the select wavelength. [c] In case of **11**, we were unable to measure the fluorescence lifetime. Because of a close structural similarity, we use the same a value as that obtained for **5**.

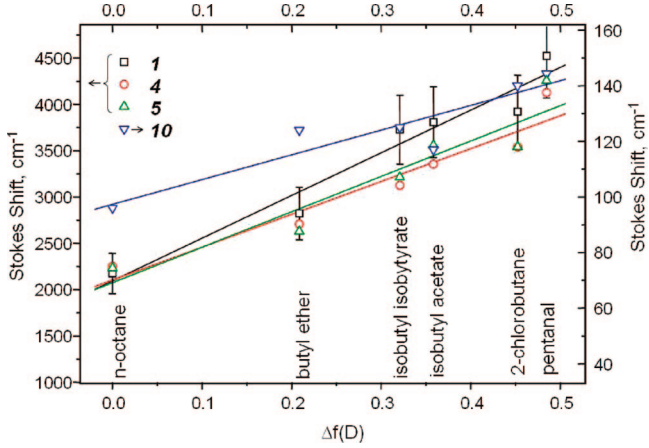

Figure 4. Solvatochromic shifts for **1**, **4**, **5** (left vertical scale), and **10** (right vertical scale) in a series of solvents. Solid lines show linear fits. Data for all other compounds are given in Table 1.

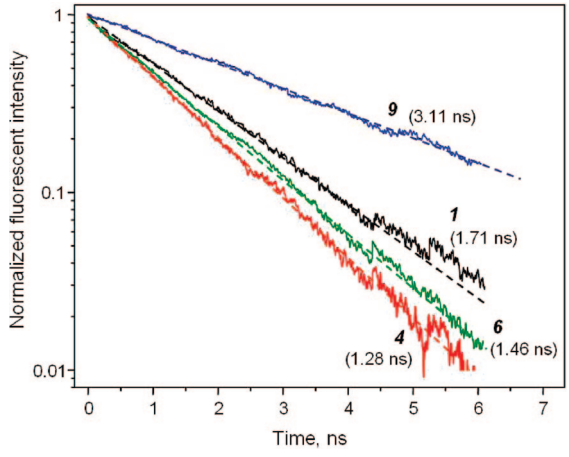

Figure 5. Fluorescence decay kinetics and corresponding single-exponential life times for **1**, **4**, **6**, and **9** in toluene. Data for all other compounds are given in Table 1.

values, corresponding to the lowest-energy component (along with the original experimental value at the same wavelength), are collected in Table 1, We estimate that σ_2^{ex} has 20% experimental error overall.

The data points that lie on top of the diagonal line represent a good coincidence between the theoretical and experimental

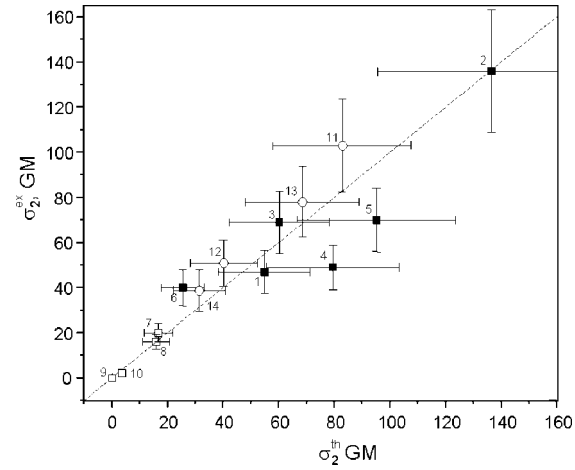

Figure 6. Comparison between the theoretically predicted cross section (horizontal axes) and that measured from the experiment (vertical axes). Solid rectangles, group i; empty rectangles, group ii; empty circles, group iii. Vertical 20% error bars are due to the experimental uncertainty in the direct measurement of σ_2^{ex}. Horizontal 30% error bars are due to the uncertainty in the determination of the dipole moment values (see the text for details).

values, whereas the data points falling far from the diagonal indicate a poor coincidence. As one can see, more than half of the data points fall into the good coincidence category. One may better quantify the degree of correlation by using the χ^2-minimization criterion

$$\chi_R^2 = \frac{1}{N-1}\sum_{i=1}^{N}\left(\frac{\sigma_i^{th}-\sigma_i^{ex}}{\Delta_i}\right)^2 \qquad (10)$$

where σ_i^{th} and σ_i^{ex}, are, correspondingly, the theoretical and the experimental cross sections, Δ_i is the standard deviation, and the summation is over all N molecules. Smaller χ_R^2 means higher correlation. For the data points shown in Figure 6, we calculate from eq 10 $\chi_R^2 = 0.15$. The same calculation with Lorentz local field model gives $\chi_R^2 = 0.21$. This justifies our preference of the Onsager model, although the correlation is very good in the other cases, too.

The circumstance that the most accurate predictions are obtained in group I may not be very surprising because the low degree of symmetry and large $\lvert\Delta\vec{\mu}_{01}\rvert$ value already indicate that the lowest-energy transition may have a strong dipolar character and is thus well described by eq 4. More noteworthy

is the fact that the simple two-level model also gives valid predictions for other systems, very much independent of the structure and symmetry properties of the molecules. For example, group ii has the lowest $|\vec{\mu}_{01}|$ and $|\Delta\vec{\mu}_{01}|$, but the theory still fits the experimental data rather well.

Of course, the current approach does not have the power to always forecast the full 2PA spectrum, and especially not the maximum 2PA value, which for many compounds (e.g., groups ii and iii) lie at higher energies. Nevertheless, our result suggests that the current method can be used to estimate the 2PA cross section of the lowest-energy transition with an accuracy comparable to that obtained in direct nonlinear absorption measurements.

6. Conclusions

We present a systematic quantitative study of the lowest-energy 2PA transition in a series of substituted diphenylaminostilbenes, push−pull porphyrins, and carbazol-substituted stilbenes. We determine the 2PA cross section value in two alternative ways: (a) by direct measurement with the femtosecond fluorescence−excitation method and (b) by using perturbation theory formula for a two-level system with a nonzero permanent dipole moment difference between the two ground and excited states. For at least half of the systems studied, the discrepancy between a and b is less than 20%, and for all molecules less than 50%. This is the first time that such direct quantitative correspondence is demonstrated for a wide range of molecules. Our result shows that relatively straightforward linear spectroscopic measurements can predict the nonlinear absorption in the lowest-energy transition with an appreciable absolute accuracy. The current approach may be extended to three- and four-level systems, provided that the higher excited-state transition and permanent dipole moments can also be obtained.

Acknowledgment. This work was supported by AFOSR Grant No. FA9550-05-1-0357.

Supporting Information Available: Synthesis and other details concerning the new compounds. This material is available free of charge via the Internet at http://pubs.acs.org.

References and Notes

(1) Zipfel, W. R.; Williams, R. M.; Webb, W. W. *Nat. Biotechnol.* **2003**, *21*, 1369–1377.

(2) Parthenopoulos, D. A.; Rentzepis, P. M. *Science* **1989**, *245*, 843–845.

(3) Strickler, J. H.; Webb, W. W. *Adv. Mater.* **1993**, *5*, 1479–481.

(4) Kawata, S.; Kawata, Y. *Chem. Rev.* **2000**, *100*, 1777–1788, and references therein.

(5) Makarov, N.; Rebane, A.; Drobizhev, M.; Wolleb, H.; Spahni, H. *JOSA B* **2007**, *24*, 1874–1885, and references therein.

(6) Cumpston, B. H.; Ananthavel, S. P.; Barlow, S.; Dyer, D. L.; Ehrlich, J. E.; Erskine, L. L.; Heikal, A. A.; Kuebler, S. M.; Lee, I.-Y.S.; McCord-Maughon, D.; Qin, J.; Rockel, H.; Rumi, M.; Wu, X.-L.; Marder, S. R.; Perry, J. W. *Nature* **1999**, *398*, 51,

(7) Spangler, C. W. *J. Mater. Chem.* **1999**, *9*, 2013–2020.

(8) Bhawalkar, J. D.; Kumar, N. D.; Zhao, C. F.; Prasad, P. N. *J. Clin. Laser Med. Surg.* **1997**, *15*, 201–204.

(9) Karotki, A.; Kruk, M.; Drobizhev, M.; Rebane, A.; Nickel, E.; Spangler, C. W. *IEEE J. Sel. Top. Quantum Electron.* **2001**, *7*, 971–975.

(10) Day, P. N.; Nguyen, K. A.; Pachter, R. *J. Phys. Chem. B* **2005**, *109*, 1803–1814.

(11) Baev, A.; Prasad, P. N. *J. Chem. Phys.* **2005**, *122*, 224309,

(12) Kogej, T.; Beljonne, D.; Meyer, F.; Perry, J. W.; Marder, S. R.; Bredas, J. L. *Chem. Phys. Lett.* **1998**, *298*, 1–6.

(13) Ferdiani, L.; Rinkevicius, Z.; Agren, H. *J. Chem. Phys.* **2005**, *122*, 244104,

(14) (a) Delysse, S.; Raimond, P.; Nunzi, J.-M. *Chem. Phys.* **1997**, *219*, 341–351. (b) Miniewicz, A.; Delysse, S.; Nunzi, J.-M.; Kajzar, F. *Chem. Phys. Lett.* **1998**, *287*, 17–21.

(15) Karotki, A. Simultaneous Two-Photon Absorption of Tetrapyrrolic Molecules: From Femtosecond Coherence Experiments to Photodynamic Therapy. Ph.D. Thesis, Montana State University, Bozeman, MT, 2003; pp 20−24, (http://www.montana.edu/etd/available/unrestricted/Karotki_03.pdf).

(16) Drobizhev, M.; Meng, F.; Rebane, A.; Stepanenko, Y.; Nickel, E.; Spangler, C. W. *J. Phys. Chem. B* **2006**, *110*, 9802–9814.

(17) Terenziani, F.; Painelli, A.; Katan, C.; Charlot, M.; Blanchard-Desce, M. *J. Am. Chem. Soc.* **2006**, *128*, 15742–15755.

(18) Drobizhev, M.; Stepanenko, Y.; Dzenis, Y.; Karotki, A.; Rebane, A.; Taylor, P. N.; Anderson, H. L. *J. Phys. Chem. B* **2005**, *109*, 7223–7236.

(19) Drobizhev, M.; Karotki, A.; Kruk, M.; Rebane, A. *Chem. Phys. Lett.* **2002**, *355*, 175–182.

(20) Drobizhev, M.; Makarov, N. S.; Stepanenko, Y.; Rebane, A. *J. Chem. Phys.* **2006**, *124*, 224701,

(21) Perez Moreno, J.; Kuzyk, M. G. *J. Chem. Phys.* **2005**, *123*, 194101.

(22) Lakowicz, J. R. *Principles of Fluorescence Spectroscopy*; Plenum Press: New York, 1983.

(23) Suppan, P. *J. Photochem. Photobiol., A* **1990**, *50*, 293–330.

(24) Pantell, R. Puthoff, H. *Fundamentals of Quantum Electronics*; John Wiley & Sons: New York, 1969.

(25) Lavoine, J. P. *J. Phys. Chem.* **2007**, *127*, 094107.

(26) Lin, T.-C.; He, G. S.; Prasad, P. N.; Tan, L.-S. *J. Mater. Chem.* **2004**, *14*, 982–991.

(27) Drobizhev, M.; Karotki, A.; Dzenis, Y.; Rebane, A.; Suo, Z. Y.; Spangler, C. W. *J. Phys. Chem. B* **2003**, *107*, 7540–7543.

(28) Drobizhev, M.; Rebane, A.; Suo, Z.; Spangler, C. W. *J. Lumin.* **2005**, *111*, 291–305.

(29) Rumi, M.; Ehrlich, J. E.; Heikal, A. A.; Perry, J. W.; Barlow, S.; Hu, Z.; McCord-Maughon, D.; Parker, T. C.; Röckel, H.; Thaymanavan, S.; Marder, S. R.; Beljonne, D.; Bredas, J.-L. *J. Am. Chem. Soc.* **2000**, *122*, 9500–9510.

(30) Makarov, N. S.; Drobizhev, M.; Rebane, A. *SPIE Proc.* **2008**, 6891.

(31) Karotki, A.; Drobizhev, M.; Kruk, M.; Spangler, C.; Nickel, E.; Mamardashvili, N.; Rebane, A. *J. Opt. Soc. Am. B* **2003**, *20*, 321–332.

(32) Shao, P.; Huang, B.; Chen, L.; Liu, Z.; Qin, J.; Gong, H.; Ding, S.; Wang, Q. *J. Mater. Chem.* **2005**, *15*, 4502–4506.

(33) Lee, S.; Thomas, K. R. J.; Thayumanavan, S.; Bardeen, C. J. *J. Phys. Chem. A* **2005**, *109*, 9767–9774.

(34) Antonov, L.; Kamada, K.; Ohta, K.; Kamounah, F. S. *Phys. Chem. Chem. Phys.* **2003**, *5*, 1193–1197.

(35) Polyutov, S.; Minkov, I.; Gel'mukhanov, F.; Agren, H. *J. Phys. Chem. A* **2005**, *109*, 9507–9513.

JP800104Q